# Supporting Information

for DOI: 10.1021/acsami.9b07275

## Tuning ZnO Sensors Reactivity Towards Volatile Organic Compounds via Ag Doping and Nanoparticle Functionalisation

Vasile Postica,[1] Alexander Vahl,[2] David Santos-Carballal,*[,3] Torben Dankwort,[4]

Lorenz Kienle,[4] Mathias Hoppe,[5] Abdelaziz Cadi-Essadek,[3] Nora H. de Leeuw,*[,3,6] Maik-Ivo Terasa,[5]

Rainer Adelung,[5] Franz Faupel,*[,2] Oleg Lupan,*[,5]

**1** Center for Nanotechnology and Nanosensors, Department of Microelectronics and Biomedical Engineering, Technical University of Moldova, 168 Stefan cel Mare Av., MD-2004 Chisinau, Republic of Moldova
**2** Chair for Multicomponent Materials, Faculty of Engineering, Institute for Materials Science, Kiel University, Kaiser str. 2, D-24143, Kiel, Germany
**3** School of Chemistry, Cardiff University, Main Building, Park Place, Cardiff CF10 3AT, United Kingdom
**4** Synthesis and Real Structure, Institute for Materials Science, Kiel University, Kaiser str. 2, D-24143, Kiel, Germany
**5** Functional Nanomaterials, Institute for Materials Science, Kiel University, Kaiserstr. 2, D-24143, Kiel, Germany
**6** Department of Earth Sciences, Utrecht University, Princetonplein 8A, 3584 CD Utrecht, The Netherlands

*Corresponding authors

| | Dr.Eng. Lupan, | Prof. Adelung | Prof. de Leeuw | Prof. Faupel |
|---|---|---|---|---|
| E-mails: | ollu@tf.uni-kiel.de<br>oleg.lupan@mib.utm.md<br>www.utm.md | ra@tf.uni-kiel.de | deLeeuwN@cardiff.ac.uk | ff@tf.uni-kiel.de |

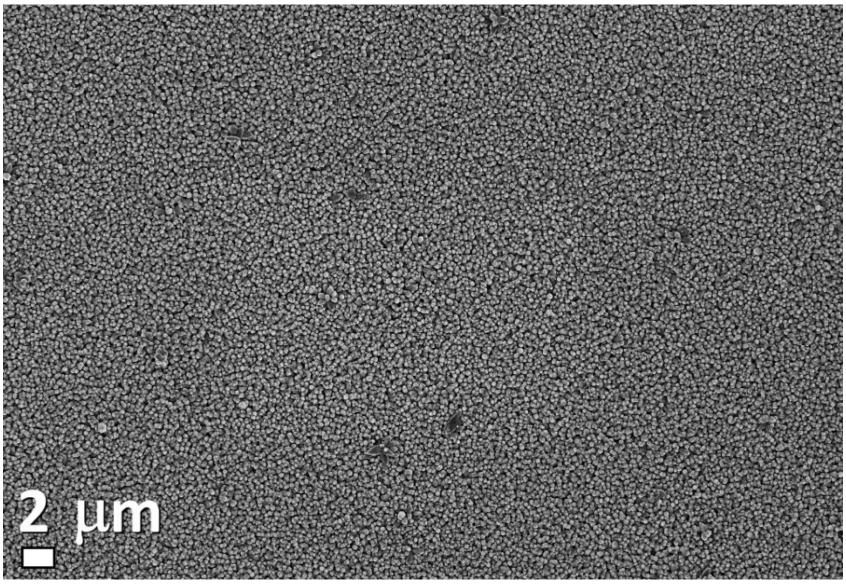


**Figure S1**. SEM image of ZnO:Ag (0.5 wt%) films treated with RTA at 575 °C for 60 s.

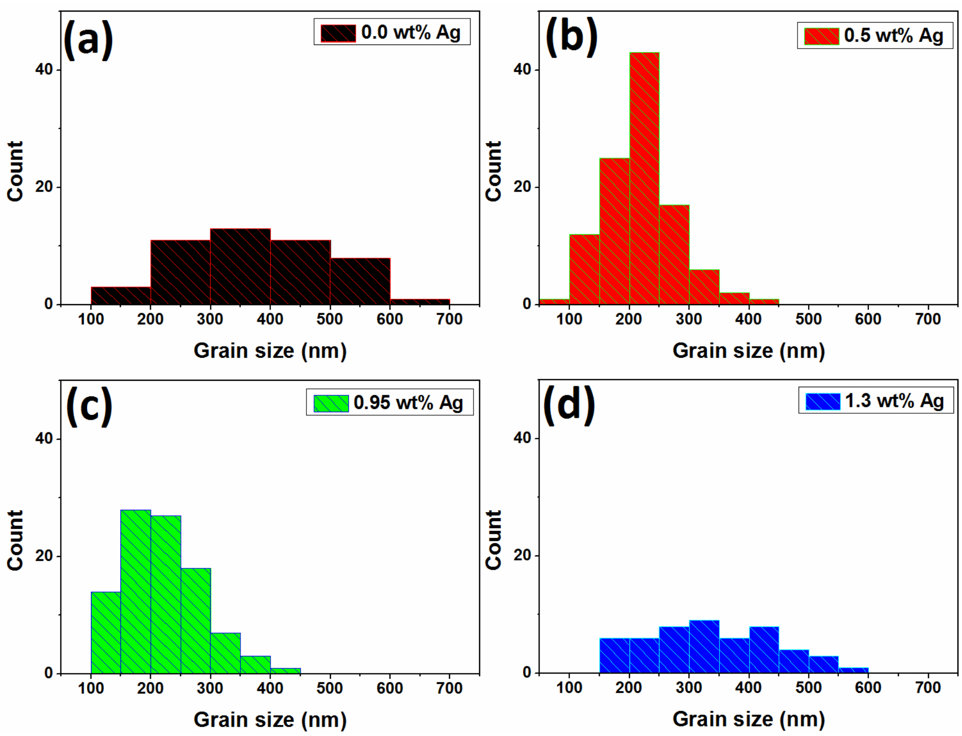


**Figure S2**. Column size histogram of ZnO:Ag columnar films with: (a) 0.00; (b) 0.50; (c) 0.95; and (d) 1.3 wt% Ag.

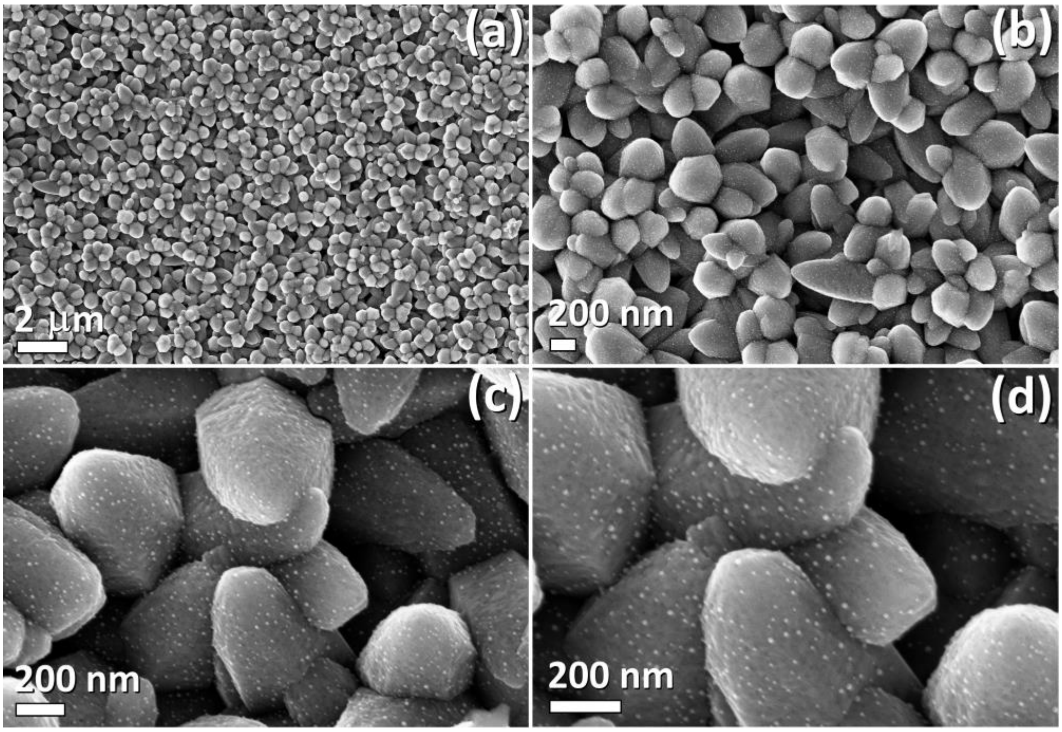


**Figure S3**. SEM images of Ag/ZnO:Ag columnar films at different magnifications from: (a,b) lower; to (c,d) higher.

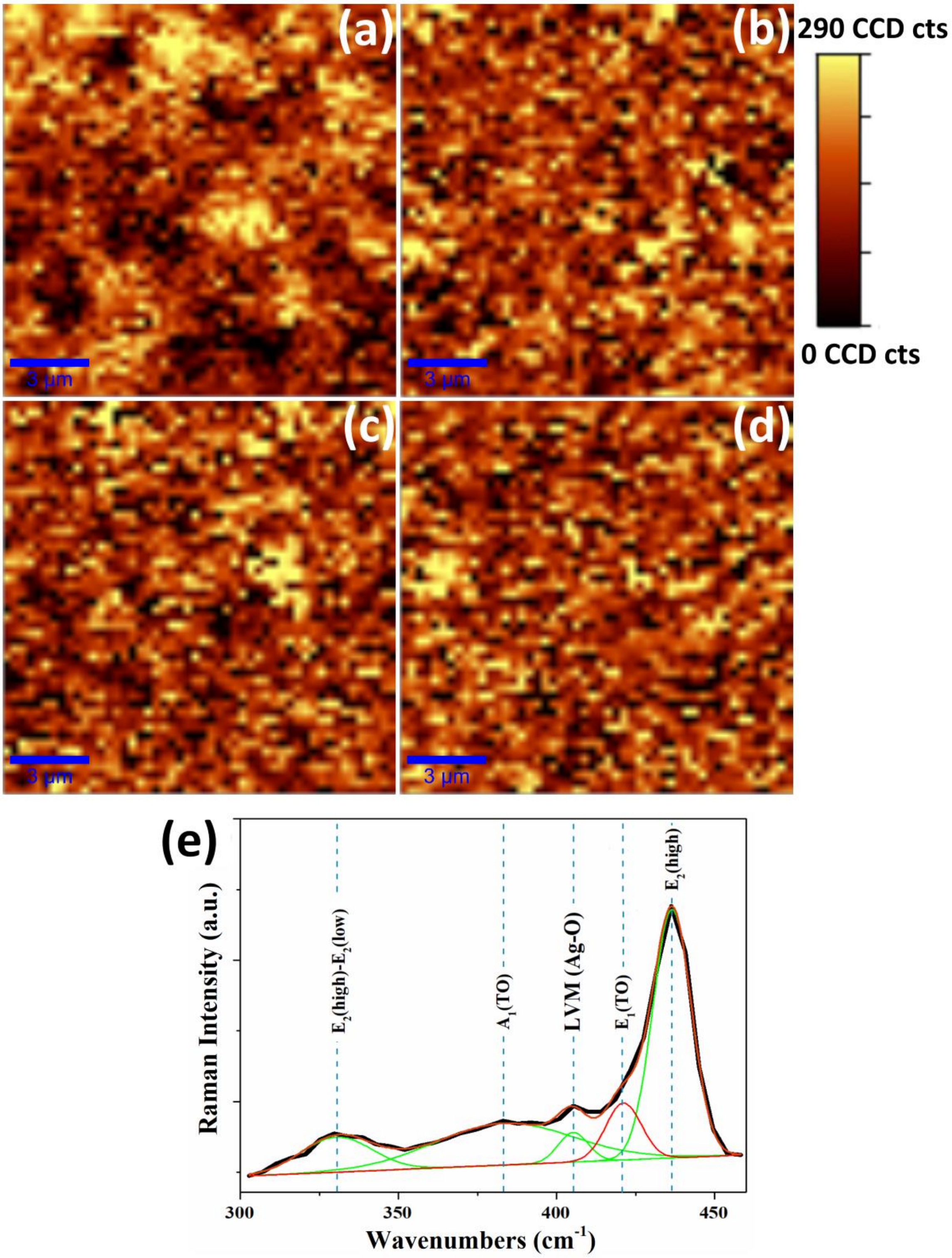


**Figure S4**. Raman mapping for the $E_2$(high) band (integrated between 420 and 450 cm$^{-1}$) of the ZnO:Ag columnar films treated with RTA at 575 ˚C for 60 s with: (a) 0.0; (b) 0.5; (c) 0.95; and (d) 1.3 wt% Ag. (e) Deconvolution of the 300-460 cm$^{-1}$ region using a Gaussian fit for the sample with 1.3 wt% Ag.

**Figure S4e** shows the deconvolution using a Gaussian fitting of the 300-460 $cm^{-1}$ Raman spectroscopy range for the sample with 1.3 wt% Ag (see **Figure S4e**). For the samples with 1.3 wt% Ag, the additional local vibrational modes (LVM) at 402 $cm^{-1}$ and 235 $cm^{-1}$ arise due to the intrinsic host lattice defects induced by the Ag atoms located in the O sites ($Ag_O$) and Zn sites ($Ag_{Zn}$), respectively, in agreement with XRD experiments.[1-4] The intensity of the LVM increases with the Ag content, which has also been reported in literature for Ag-doped ZnO films.[5,6] A plausible mechanism to account for the origin of the LVM peak comprises Ag impurity centers breaking the translational symmetry of the ZnO crystal which relaxes the conservation of the wave vectors, allowing them far from the dopant center.[3,6]

**Equation (S1)** gives the estimated Ag-related LVM frequency from the effective masses [$\mu = (1/M + 1/m)^{-1}$] of the ZnO and LVM:[6,7]

$$\frac{\omega(LVM)}{\omega(ZnO)} = \sqrt{\frac{\mu_{ZnO}}{\mu_{LVM}}} \qquad \text{(S1)}$$

From $\omega(\text{ZnO}) = \omega[E_2(\text{high})] = 436$ $cm^{-1}$ we obtained the value of 245 $cm^{-1}$ for $Ag_O$ (LVM of Zn-Ag). The calculated frequency of the LVM for the Ag–Zn pair is consistent with the experimental value of 235 $cm^{-1}$, confirming that this signal is induced by the Ag atoms located in the Zn sites of the ZnO lattice.[6,7] In the same way, the mode at 402 $cm^{-1}$ is the LVM induced by the Ag atoms located in the O sites of the ZnO lattice.[6,7] **Figure S4e**, shows that the relative intensity of the LVM peaks for Zn-Ag is higher than for Ag-O, strongly suggesting that Ag mainly replace Zn atoms.[6,7,8]

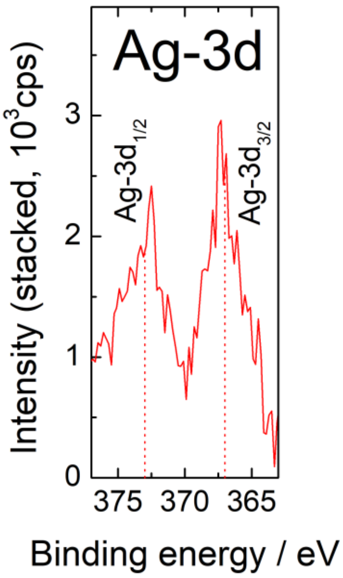


**Figure S5**. XPS plot of the Ag-3d lines of a ZnO:Ag reference layer with increased (10-fold) Ag doping concentration (123 mM of $AgNO_3$).

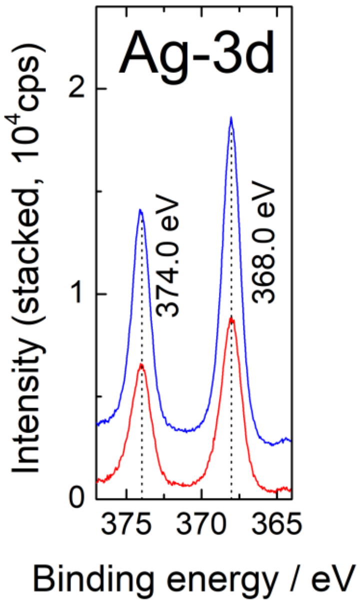


**Figure S6**. XPS plot of the Ag-3d lines of a ZnO:Ag films with Ag nanoclusters as-grown (red line) and annealed ones at 300 ºC for 1 h (blue line).

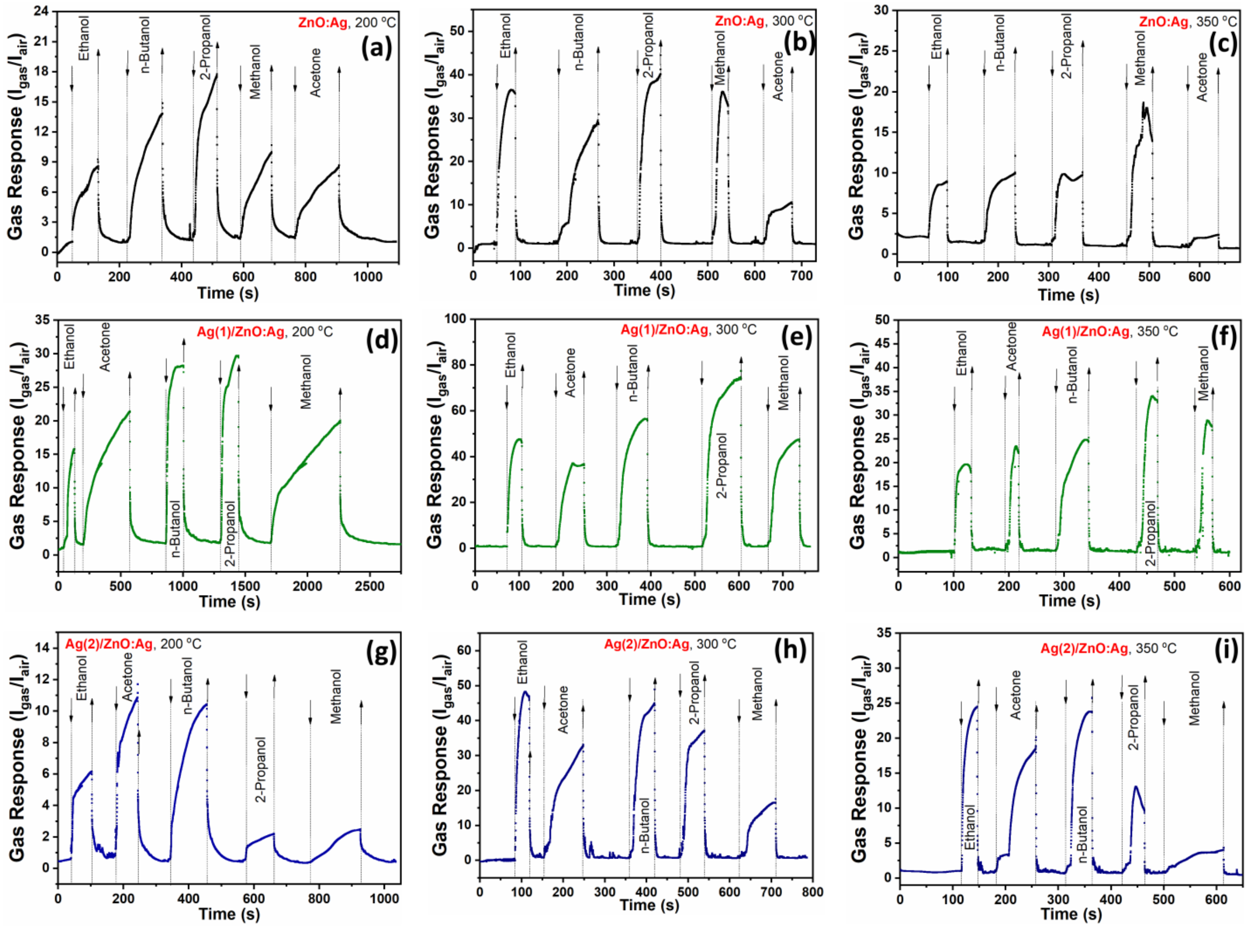


**Figure S7**. Dynamic response to 100 ppm of VOC vapors for: ZnO:Ag films based sensor structures at: (a) 200 °C, (b) 300 °C and (c) 350 °C; Ag(1)/ZnO:Ag at: (d) 200 °C, (e) 300 °C and (f) 350 °C, and Ag(2)/ZnO:Ag at: (g) 200 °C, (h) 300 °C and (i) 350 °C.

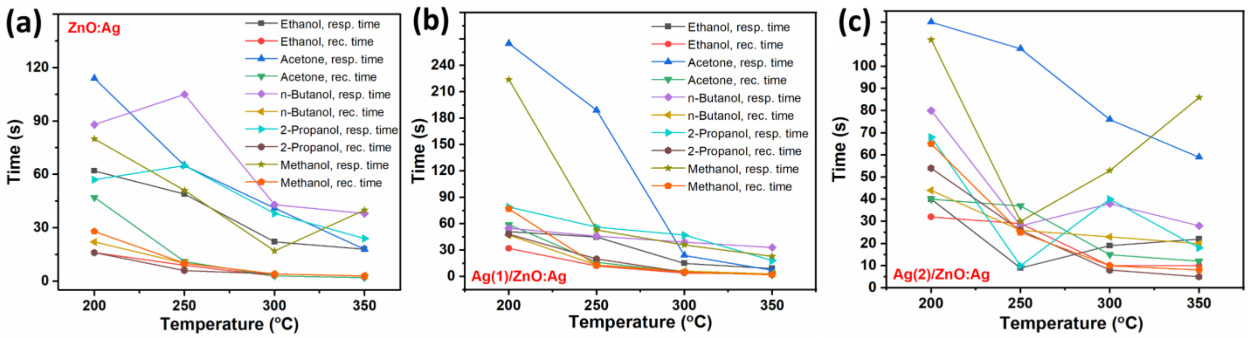


**Figure S8**. Calculated response (resp.) and recovery times (rec.) as a function of temperature for: (a) ZnO:Ag, (b) Ag(1)/ZnO:Ag and (c) Ag(2)/ZnO:Ag columnar films based sensor structures.

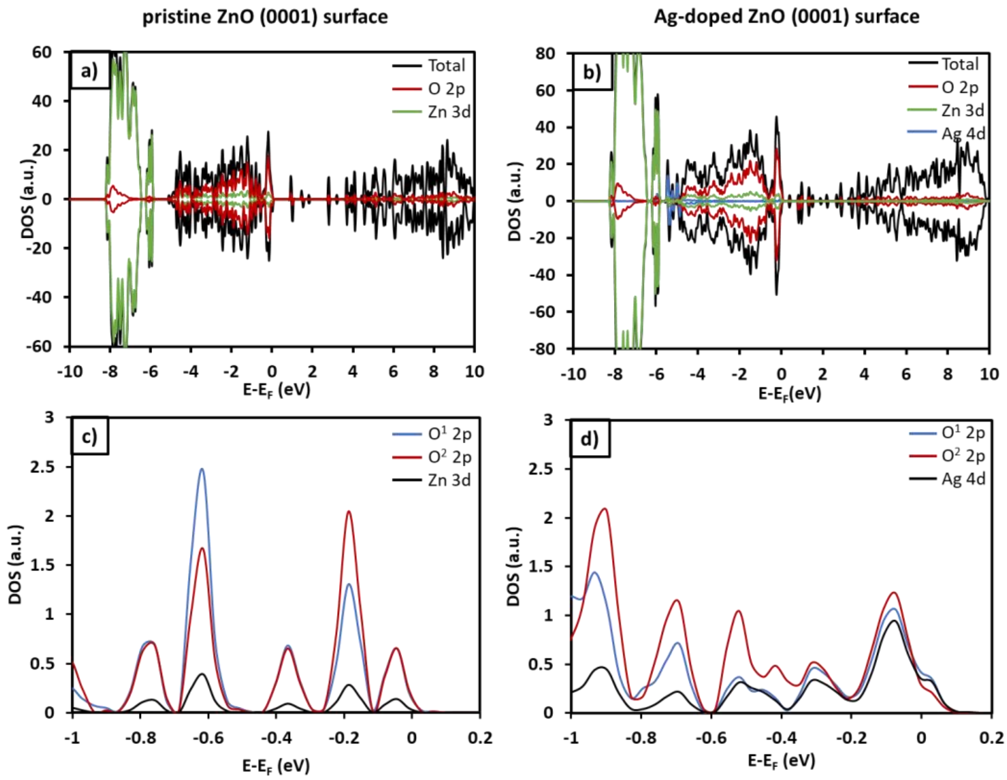


**Figure S9.** (a and b) Electronic density of states (DOS) of the pristine and Ag-doped ZnO(0001) surfaces, respectively. (c and d) Atomic projected DOS of the pristine and Ag-doped ZnO(0001) surfaces, respectively.

**Table S1**. Calculated response and recovery times to VOCs vapors at different operating temperatures for columnar films based sensor structures.

| Sample | VOCs | Time | Temperature, $^0$ C | | | |
|---|---|---|---|---|---|---|
| | | | **200** | **250** | **300** | **350** |
| **ZnO:Ag** | *Ethanol* | Resp. time (s) | 62 | 49 | 22 | 18 |
| | | Rec. time (s) | 16 | 9 | 3 | 2 |
| | *Acetone* | Resp. time (s) | 114 | 65 | 41 | 18 |
| | | Rec. time (s) | 47 | 11 | 3 | 2 |
| | *n-Butanol* | Resp. time (s) | 88 | 105 | 43 | 38 |
| | | Rec. time (s) | 22 | 10 | 4 | 3 |
| | *2-Propanol* | Resp. time (s) | 57 | 65 | 38 | 24 |
| | | Rec. time (s) | 16 | 6 | 4 | 3 |
| | *Methanol* | Resp. time (s) | 80 | 51 | 17 | 40 |
| | | Rec. time (s) | 28 | 10 | 4 | 3 |
| **Ag(1)/ZnO:Ag** | *Ethanol* | Resp. time (s) | 51 | 45 | 15 | 9 |
| | | Rec. time (s) | 32 | 12 | 4 | 3 |
| | *Acetone* | Resp. time (s) | 265 | 189 | 24 | 7 |
| | | Rec. time (s) | 59 | 16 | 5 | 2 |
| | *n-Butanol* | Resp. time (s) | 55 | 46 | 39 | 33 |
| | | Rec. time (s) | 47 | 13 | 6 | 3 |
| | *2-Propanol* | Resp. time (s) | 79 | 56 | 47 | 18 |
| | | Rec. time (s) | 48 | 20 | 5 | 2 |
| | *Methanol* | Resp. time (s) | 224 | 53 | 36 | 23 |
| | | Rec. time (s) | 77 | 13 | 5 | 2 |
| **Ag(2)/ZnO:Ag** | *Ethanol* | Resp. time (s) | 40 | 9 | 19 | 22 |
| | | Rec. time (s) | 32 | 29 | 10 | 10 |
| | *Acetone* | Resp. time (s) | 120 | 108 | 76 | 59 |
| | | Rec. time (s) | 40 | 37 | 15 | 12 |
| | *n-Butanol* | Resp. time (s) | 80 | 28 | 38 | 28 |
| | | Rec. time (s) | 44 | 26 | 23 | 20 |
| | *2-Propanol* | Resp. time (s) | 68 | 10 | 40 | 18 |
| | | Rec. time (s) | 54 | 26 | 8 | 5 |
| | *Methanol* | Resp. time (s) | 112 | 30 | 53 | 86 |
| | | Rec. time (s) | 65 | 25 | 10 | 8 |

**Table S2**. Calculated gas response and detection limit to VOCs vapors at 250 ºC operating temperature for columnar films based sensor structures.

| **Sample** | **VOCs** | **VOC conc. (ppm)** | **Gas Response ($I_{gas}/I_{air}$)** | **Detection limit (ppm)** |
|---|---|---|---|---|
| ZnO:Ag | *Ethanol* | 10 | 8.5 ± 1.6 | 0.48 ± 0.05 |
| | | 50 | 18.6 ± 1.9 | |
| | | 100 | 30.8 ± 3.1 | |
| | | 500 | 89 ± 6.8 | |
| | *Acetone* | 10 | 4.9 ±1.8 | 0.66 ± 0.08 |
| | | 50 | 11.5 ± 2.1 | |
| | | 100 | 16.5 ± 2.2 | |
| | | 500 | 39 ± 3.6 | |
| | *n-Butanol* | 10 | 12 ± 1.2 | 0.22 ± 0.02 |
| | | 50 | 29 ± 2.1 | |
| | | 100 | 40.8 ± 3.5 | |
| | | 500 | 98 ± 6.8 | |
| | *2-Propanol* | 10 | 15.3 ± 1.2 | 0.13 ± 0.01 |
| | | 50 | 36 ± 3.1 | |
| | | 100 | 52.5 ± 4.8 | |
| | | 500 | 115 ± 7.1 | |
| | *Methanol* | 10 | 8.9 ± 2.1 | 0.06 ± 0.02 |
| | | 50 | 23 ± 2.5 | |
| | | 100 | 31 ± 2.6 | |
| | | 500 | 73 ± 3.8 | |
| Ag(1)/ZnO:Ag | *Ethanol* | 10 | 19 ± 1.6 | 0.1 ± 0.01 |
| | | 50 | 42 ± 2.9 | |
| | | 100 | 74.3 ± 5.8 | |
| | | 500 | 189 ± 10.1 | |
| | *Acetone* | 10 | 12 ± 1.5 | 0.17 ± 0.02 |
| | | 50 | 32 ± 2.5 | |
| | | 100 | 48.5 ± 3.8 | |
| | | 500 | 112 ± 6.9 | |
| | *n-Butanol* | 10 | 15 ± 1.6 | 0.21 ± 0.03 |
| | | 50 | 35 ± 2.6 | |
| | | 100 | 66.7 ± 3.9 | |
| | | 500 | 175 ± 5.8 | |
| | *2-Propanol* | 10 | 25 ± 2. | 0.05 ± 0.01 |
| | | 50 | 51 ± 3.6 | |
| | | 100 | 82 ± 4.8 | |
| | | 500 | 201 ± 6.9 | |
| | *Methanol* | 10 | 8.5 ± 1.6 | 0.37 ± 0.05 |
| | | 50 | 23 ± 2.1 | |
| | | 100 | 32.3 ± 3.5 | |
| | | 500 | 85 ± 4.8 | |
| Ag(2)/ZnO:Ag | *Ethanol* | 10 | 36 ± 2.5 | 0.02 ± 0.01 |
| | | 50 | 85 ± 4.8 | |
| | | 100 | 145 ± 9.8 | |
| | | 500 | 355 ± 22 | |
| | *Acetone* | 10 | 23 ± 1.5 | 0.07 ± 0.02 |
| | | 50 | 63 ± 3.8 | |
| | | 100 | 100 ± 5.8 | |
| | | 500 | 281 ± 21 | |
| | *n-Butanol* | 10 | 39 ± 1.8 | 0.04 ± 0.01 |
| | | 50 | 102 ± 5.6 | |
| | | 100 | 156 ± 6.8 | |
| | | 500 | 405 ± 32 | |
| | *2-Propanol* | 10 | 46 ± 3.8 | 0.01 ± 0.005 |
| | | 50 | 118 ± 9.8 | |
| | | 100 | 175 ± 10.2 | |
| | | 500 | 439 ± 23 | |
| | *Methanol* | 10 | 13 ± 1.1 | 0.24 ± 0.05 |
| | | 50 | 32 ± 2.5 | |
| | | 100 | 54 ± 3.5 | |
| | | 500 | 145 ± 9.5 | |

**Table S3**. Calculated gas response to VOCs vapors at 250 ºC operating temperature under different values of RH.

| Sample | VOCs | Gas Response ($I_{gas}/I_{air}$) | |
|---|---|---|---|
| | | **RH 30%** | **RH 85%** |
| ZnO:Ag | *Ethanol* | 30.8 ± 2 | 16 ± 2 |
| | *Acetone* | 16.5 ± 1 | 8.3 ± 0.9 |
| | *n-Butanol* | 40.8 ± 2.5 | 22 ± 1.5 |
| | *2-Propanol* | 52.5 ± 3.5 | 28.3 ± 1.9 |
| | *Methanol* | 31 ± 3 | 15 ± 1.1 |
| | *Hydrogen* | 2.1 ± 0.5 | 1.3 ± 0.1 |
| Ag(1)/ZnO:Ag | *Ethanol* | 74.3 ± 5.2 | 53 ± 2.8 |
| | *Acetone* | 48.5 ± 4.1 | 39 ± 3.1 |
| | *n-Butanol* | 66.7 ± 5.2 | 51 ± 5 |
| | *2-Propanol* | 82 ± 6.5 | 63 ± 5.1 |
| | *Methanol* | 32.3 ± 1.5 | 26 ± 1.8 |
| | *Hydrogen* | 1.5 ± 0.1 | 1.4 ± 0.1 |
| Ag(2)/ZnO:Ag | *Ethanol* | 145 ± 12.5 | 132 ± 8.9 |
| | *Acetone* | 100 ± 8 | 89 ± 6.5 |
| | *n-Butanol* | 156 ± 9 | 143 ± 9.8 |
| | *2-Propanol* | 175 ± 10 | 157 ± 8.5 |
| | *Methanol* | 54 ± 2.9 | 50 ± 4.5 |
| | *Hydrogen* | 1.69 ± 0.1 | 1.6 ± 0.1 |

## Author contributions

O. L., V. P., and A. V. synthesized the Ag-functionalized ZnO:Ag material. O. L. developed synthesis from chemical solution procedure SCS for ZnO. O. L., V. P., A. V., M.-I. T. and M. H. adapted technological approach for material synthesis and integration/fabrication of the sensors. A. V. and F. F. developed functionalization procedure, set-up and realized all experiments and XPS analysis. P. V. and O. L. carried out the measurement of sensing properties of sensors based on such structures and analyzed data. T. D. and L. K. studied TEM. V. P., O. L., M. H., R. A., M.-I. T. analyzed the results, including Raman data and revised draft. N. H.d.L., D. S.-C. and A. C. -E. realized computational part. A. V., P. V., A. C. -E., D. S.-C., R. A and O. L. drafted the article. O. L., F. F., N. H.d.L., L. K. and R. A. conceived and designed the study and approved the final version of the manuscript to be published. All authors reviewed the manuscript.

## Conflicts of interest

There are no conflicts to declare.

## Acknowledgements

Dr. Lupan acknowledges the Alexander von Humboldt Foundation for the research fellowship for experienced researchers 3-3MOL/1148833 STP at the Institute for Materials Science, Kiel University, Germany. This research was sponsored partially by the German Research Foundation (DFG) through the research unit FOR2093. This research was partly supported by the STCU and ASM within the Grant 6229A. We acknowledge the Engineering and Physical Sciences Research Council (EPSRC grant EP/K009567) for funding. Via our membership of the UK's HEC Materials Chemistry Consortium, which is funded by EPSRC (EP/L000202), this work used the ARCHER UK National Supercomputing Service (http://www.archer.ac.uk). This work was performed using the computational facilities of the Advanced

Research Computing @ Cardiff (ARCCA) Division, Cardiff University. The authors also acknowledge the use of HPC Wales, Supercomputing Wales and associated support services in the completion of this work. All data created during this research is openly available from the Cardiff University's Research Portal at http://doi.org/10.17035/d.2019.0081497456.

## References

(1) Jeong, S. H.; Park, B. N.; Lee, S. B.; Boo, J. H. Structural and Optical Properties of Silver-Doped Zinc Oxide Sputtered Films. *Surf. Coat. Technol.* **2005,** *193*, 340-344.

(2) Lupan, O.; Chow, L.; Ono, L. K.; Cuenya, B. R.; Chai, G.; Khallaf, H.; Park, S.; Schulte, A. Synthesis and Characterization of Ag- or Sb-Doped ZnO Nanorods by a Facile Hydrothermal Route. *J. Phys. Chem. C* **2010,** *114*, 12401-12408.

(3) Tringe, J. W.; Levie, H. W.; McCall, S. K.; Teslich, N. E.; Wall, M. A.; Orme, C. A.; Matthews, M. J. Enhanced Raman Scattering and Nonlinear Conductivity in Ag-Doped Hollow ZnO Microspheres. *Appl. Phys. A* **2012,** *109*, 15-23.

(4) Zeferino, R. S.; Flores, M. B.; Pal, U. Photoluminescence and Raman Scattering in Ag-Doped ZnO Nanoparticles. *J. Appl. Phys.* **2011,** *109*, 014308.

(5) Bian, H. Q.; Ma, S. Y.; Zhang, Z. M.; Gao, J. M.; Zhu, H. B. Microstructure and Raman Scattering of Ag-Doping ZnO Films Deposited on Buffer Layers. *J. Cryst. Growth* **2014,** *394*, 132-136.

(6) Wang, X. B.; Song, C.; Geng, K. W.; Zeng, F.; Pan, F. Luminescence and Raman Scattering Properties of Ag-Doped ZnO Films. *J. Phys. D, Appl. Phys.* **2006,** *39*, 4992.

(7) Ye, J. D.; Gu, S. L.; Zhu, S. M.; Liu, S. M.; Zheng, Y. D.; Zhang, R.; Shi, Y.; Chen, Q.; Yu, H. Q.; Ye, Y. D. Raman Study of Lattice Dynamic Behaviors in Phosphorus-Doped ZnO Films. *Appl. Phys. Lett.* **2006,** *88*, 101905.

(8) Lupan, O.; Chow, L.; Shishiyanu, S.; Monaico, E.; Shishiyanu, T.; Şontea, V.; Cuenya, B. R.; Naitabdi, A.; Park, S.; Schulte, A. Nanostructured zinc oxide films synthesized by successive chemical solution deposition for gas sensor applications. *Mater. Res. Bull*. **2009**, *44*, 63-69.